

**Paper 54-4** has been designated as a Distinguished Paper at Display Week 2022. The full-length version of this paper appears in a Special Section of the *Journal of the Society for Information Display (JSID)* devoted to Display Week 2022 Distinguished Papers. This Special Section will be freely accessible until December 31, 2022 via:

[https://sid.onlinelibrary.wiley.com/doi/toc/10.1002/\(ISSN\)1938-3657.DW22](https://sid.onlinelibrary.wiley.com/doi/toc/10.1002/(ISSN)1938-3657.DW22)

Authors that wish to refer to this work are advised to cite the full-length version by referring to its DOI:

<https://sid.onlinelibrary.wiley.com/doi/10.1002/jsid.1122>



# Low-Diffraction Transparent $\mu$ LED Displays with Optimized Pixel Structure

Qian Yang,<sup>1</sup> Zhiyong Yang,<sup>1</sup> Yi-Fen Lan,<sup>2</sup> and Shin-Tson Wu<sup>1</sup>

<sup>1</sup>College of Optics and Photonics, University of Central Florida, Orlando, FL

<sup>2</sup>AU Optronics Corp., Hsinchu Science Park, Hsinchu, Taiwan

## Abstract

*A semi-analytical model is built based on diffraction theory and human angular resolution to quantitatively evaluate the diffraction effect of transparent displays, including micro-LED and OLED. By optimizing the pixel structures within a  $2 \times 2$ -pixel size region, the relative diffraction intensity is reduced by 42% at the 50% aperture ratio regardless of pixel density.*

## Author Keywords

transparent display; under-display camera; micro-LED; diffraction suppression; pixel structure optimization

## 1. Introduction

Transparent display is a promising technology with potential applications in smart windows, automotive windshield displays, Under-Display Cameras, Under-Display Sensors as well as augmented reality displays for showcase [1,2], to name a few. The emerging micro-LED technology [3] is a promising solution for transparent displays because of its high brightness and large aperture ratio due to small chip size and its inorganic emissive nature [4]. Sony has successfully developed a tiled 16K micro-LED screen with 99% aperture ratio, which shows an outstanding ambient contrast ratio [5], although the pixel per inch is only about 20. For automotive applications, clear and vivid images from display itself (foreground) and the scene after display (background) are both desired. Yet, the see-through images are often blurred caused by light diffraction after passing through the periodic pixel structures [6]. Our study shows that the image quality deteriorates more if the objects are far away from the display, which is a common situation while driving. For smartphone applications, people are pursuing full-screen designs with high pixel density to enhance the interaction between users and devices by eliminating the need for bezels to improve the screen-to-body ratio. Under-display camera is a new trend to achieve a sleek industrial design but mounting the display in front of a camera will also cause severe image degradation. Deep learning related algorithms are adopted to restore the blurred images by modelling different optical effects caused by the display, camera lens and human vision system, but real-time algorithms are hard to be applied in preview and video mode currently [7]. Thus, it is of great importance to suppress the diffraction effect from the viewpoint of optics, especially for devices with high pixel density where a high aperture ratio is challenging for panel fabrication. Transparent display is essentially a binary aperture function from the viewpoint of diffraction theorem, where the transmittance is 1 in open regions and 0 in opaque regions. Tsai et al. [8] studied the diffraction widths with a Gaussian beam passing through apertures with different pixel structures and assumed that a narrower diffraction width could mitigate the diffraction effect. This assumption does not take human factors into account so that the result might lead to some uncertainty due to the finite aperture size (on the order of millimeters). Qin et al. [9] proposed to simulate diffracted see-through images and evaluate the pixel structures with subjective image quality score. To our knowledge, no simple, reference-image independent and physically intuitive evaluation

methodology is proposed for the diffraction effect of transparent displays with human factors considered. In this paper, we first build our quantitative evaluation method for the diffraction effect perceived by human eyes and then analyze the magnitude of diffraction in conventional pixel structure with various object distances, resolutions, and aperture ratios. A pixel structure optimization method is introduced to minimize the diffraction effect for transparent displays with a small aperture ratio.

## 2. Theory

The point spread function (PSF) is the response of an incoherent imaging system to a point source input and blurred images can be obtained by convolution of the objects and the PSF. Thus, by studying the PSF of an imaging system including a transparent display and a human eye, one can investigate the diffraction effect of pixel structures to humans. In Figure 1, the schematics of the imaging system is illustrated and light from background objects propagates in free space for  $d_1$  and pass through the transparent display. A human eye is modeled as a positive lens with focal length  $f$ , positioned at  $d_2$  after the transparent display, and the imaging plane is located on the retina.

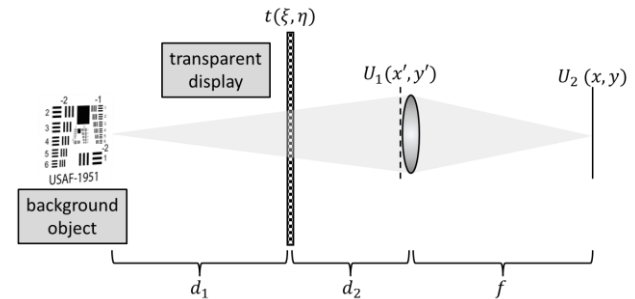


Figure 1. The schematics of the imaging system.

The derivation of the PSF with a finite object distance  $d_1$  is shown in [9] and the system PSF on the retina can be expressed as follows:

$$h(x, y) \propto \left| \mathcal{F} \{ t(\xi, \eta) \} \Big|_{f_x = \frac{x}{\lambda M f}, f_y = \frac{y}{\lambda M f}} \right|^2, \quad (1)$$

where  $f_x$  and  $f_y$  is the spatial frequency in  $x$ ,  $y$  direction,  $\lambda$  is the wavelength, and script letter  $F$  is the symbol for Fourier Transform (FT). In Equation (1), the finite pupil size of human eye is ignored since this study focuses on diffraction from the display panel. In this imaging system, the PSF  $h(x, y)$  is the modulus square of FT of the aperture distribution  $t(\xi, \eta)$ . The focal length  $f$  is about 17mm for distant objects, which is almost equivalent to the distance from pupil to retina. Parameter  $M = d_1 / (d_1 + d_2)$  is a metric for relative object distance from the transparent display and  $M = 1$  when the object is at infinity. The transparent display is regarded as a 2D aperture function  $t(\xi, \eta)$ , where amplitude transmittance is defined as either 0 (opaque) or 1 (transparent) at each point. The opaque area includes the emitting unit and the circuits, and the rest area is transparent. In

Fourier optics, the display panel with periodic pixel arrangement can be modeled as a 2D grating as it redistributes incident light into various diffraction orders. Therefore, following the convention in [6], the aperture function  $t(\xi, \eta)$  can be modeled by convolution between a unit cell function  $t_0(\xi, \eta)$  and a comb function and constrained by finite boundaries represented by a rectangular function, as shown in Equation (2),

$$t(\xi, \eta) = \left[ t_0(\xi, \eta) \otimes \text{comb}\left(\frac{\xi}{L_{x0}}, \frac{\eta}{L_{y0}}\right) \right] \times \text{rect}\left(\frac{\xi}{L_x}\right) \text{rect}\left(\frac{\eta}{L_y}\right), \quad (2)$$

where  $L_{x0}$  and  $L_{y0}$  are the size of the unit cell, and  $L_x$  and  $L_y$  are the actual size of the display panel. Its FT can be expressed as:

$$h(x, y) \propto \left[ \begin{aligned} & \left[ h_0(f_x, f_y) \times \text{comb}(L_{x0}f_x, L_{y0}f_y) \right]^2 \\ & \otimes \text{sinc}(L_x f_x) \text{sinc}(L_y f_y) \end{aligned} \right]_{f_x = \frac{x}{\lambda Mf}, f_y = \frac{y}{\lambda Mf}}, \quad (3)$$

where  $h_0(f_x, f_y)$  is the FT of  $t_0(\xi, \eta)$ .

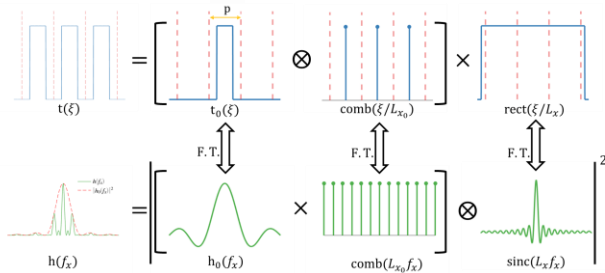


**Figure 2.** A visual representation of PSF calculation in an imaging system including a transparent display. For simplicity, 1D derivation is shown here but it is easy to extend to two dimensions.

In Figure 2, an intuitive demonstration of how to efficiently calculate the system PSF is shown, where the FT of unit cell function  $t_0(\xi, \eta)$  can be solved numerically and then PSF  $h(x, y)$  is analytically obtained. In this way, tremendous computational load is greatly relieved, while accurate PSF is still guaranteed. The comb function in PSF expression indicates the spacing between diffraction order on the retina is  $M\lambda f/L_{x0}$  and  $M\lambda f/L_{y0}$  in  $x$  and  $y$  direction and the sinc function means that each diffraction order has a finite diffraction width  $M\lambda f/L_x$  and  $M\lambda f/L_y$ . The angular resolution of human eyes is 1 arcminute and its corresponding length on the retina is  $5\mu\text{m}$ . Since the energy mainly concentrates in the zeroth diffraction order, located in the center of imaging plane, and gradually wears off in the higher orders, it is reasonable to assume that only diffraction orders that are  $5\mu\text{m}$  away from the zeroth order can be distinguished by the eye. Those closer diffraction orders are blended with zeroth order, undistinguishable to humans. Therefore,  $5\mu\text{m}$  away from the zeroth order, the relative maximum diffraction intensity, quantitatively characterizes the magnitude of diffraction effect of transparent display to human eyes, where zeroth order intensity is normalized to 1. The diffraction width of the sinc function is about tens of nanometers or less for a display panel with  $10^3 \sim 10^4$  pixels in each dimension, which is relatively small compared with human eye resolution and thus can be ignored in the PSF calculation. That means the system PSF can be simplified as a comb function modulated by FT of unit cell function  $t_0(\xi, \eta)$ .

### 3. Conventional pixel structures

In conventional pixel structures, the positions of the opaque region in each pixel are the same. The impact of object distance, panel resolution and pixel aperture ratio on the diffraction effect to human eyes is analyzed by our model. Without losing generality, we assume the pixel geometry is square with side length  $p$  and the opaque region geometry is square, located in the center of each pixel, since the diffraction effect is reported to be irrelevant to pixel/opaque geometry [9]. The size of opaque region  $b$  is determined by the aperture ratio  $\alpha$ , proportional to the square root of  $1-\alpha$ . Noticing that the spacing between diffraction orders is proportional to the parameter  $M$ . If  $M$  is small, the PSF is scaled down and most energy is within  $5\mu\text{m}$  from the zeroth diffraction order, so there is no visible diffraction effect. Hence, the diffraction effect is most obvious when object is at infinity ( $M = 1$ ) and the following analysis are taken under this extreme scenario.

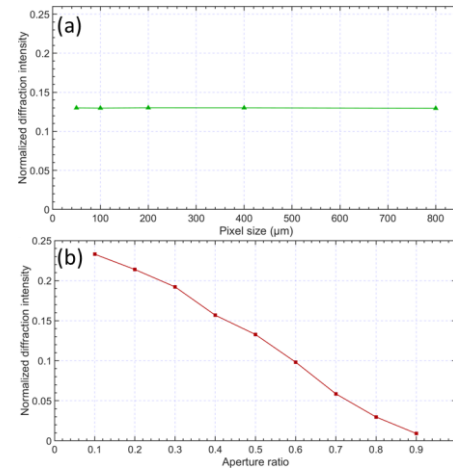


**Figure 3.** (a) At aperture ratio  $\alpha=50\%$ , the relative diffraction intensity is invariant to the pixel size  $p=50\sim 800\mu\text{m}$ . (b) With pixel size  $p=400\mu\text{m}$ , the normalized diffraction intensity decreases as aperture ratio  $\alpha$  goes from 10% to 90%.

The panel resolution is determined by the pixel size. For common display devices, the pixel sizes are usually tens of microns to hundreds of microns. In Figure 3(a), the aperture ratio is set to  $\alpha=50\%$  and the relative diffraction intensity is invariant to the pixel size. The result seems counter-intuitive at the first glance since diffraction effect is generally more obvious with finer structure. This result coincides with the conclusion in [9], by evaluating the subjective score of see-through images. From Equation (3), the pixel size only impacts the coordinate transformation in the PSF calculation and the diffraction order spacing is inversely proportional to the size of unit cell, equal to or larger than the pixel size. Even with an unrealistically large pixel size  $p=1000\mu\text{m}$ , the order spacing is  $9.35\mu\text{m}$  at green light ( $\lambda=550\text{nm}$ ), larger than human eye's angular resolution, leading to the same diffraction intensity observed by human eye for pixel sizes vary from  $50\sim 800\mu\text{m}$  in Figure 3(a).

Another important impact factor is the aperture ratio. In Figure 3(b), the pixel sizes are set to be  $400\mu\text{m}$ , and the normalized diffraction intensity decreases as the aperture ratio increases from 10% to 90%. According to the similarity theorem of FT, the open region is stretched at higher aperture ratio and its PSF is squeezed, leading to a lower diffraction intensity. It seems that boosting the aperture ratio of pixels is the only way to suppress

diffraction effect in the conventional pixel structures. The aperture ratio is directly related to the chip size of LED. However, even with micro-LED technology, it is hard to achieve large aperture ratio while maintaining high resolution with current fabrication technologies. It would be of practical interest to industry if the diffraction effect could be reduced at a relatively small aperture ratio.

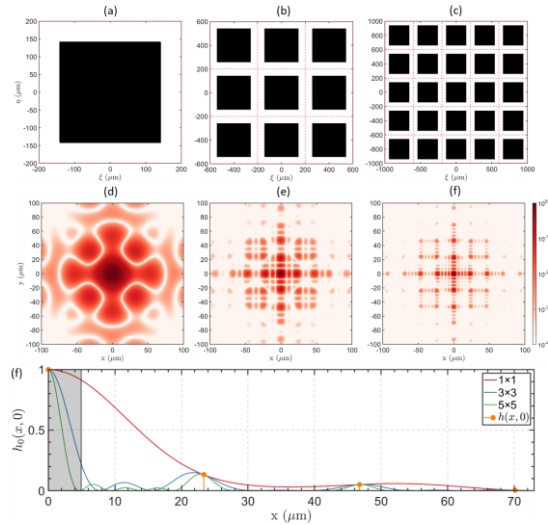


**Figure 4.** (a-c) With pixel size  $p=400\mu\text{m}$  and aperture ratio  $\alpha=50\%$ , unit cell functions  $t_0(\xi, \eta)$  with  $1\times 1$ ,  $3\times 3$ ,  $5\times 5$  pixels in one unit cell for conventional pixel structures. (d-f) FTs of unit cell functions in Figure 4(a-c). (f) The horizontal cross-section  $h_0(x, y)$  excerpted from Figure 4(d-f).

#### 4. Optimized pixel structures

In Figure 2, the size of unit cell function  $t_0(\xi, \eta)$  is the same as the pixel size, but in fact, the unit cell could include more pixels and final PSF will be the same for conventional pixel structures. With  $p=400\mu\text{m}$  and  $\alpha=50\%$ , Figure 6(a-c) shows  $t_0(\xi, \eta)$  with  $1\times 1$ ,  $3\times 3$ ,  $5\times 5$  pixels in one unit cell, respectively, and their FT  $h_0(x, y)$  in Figure 6(d-c) looks quite different. Figure 6(f) shows their horizontal cross section  $h_0(x, 0)$  and they both converge to the same PSF  $h(x, 0)$ , multiplying by comb functions with corresponding diffraction order spacing. After all, in conventional pixel structures, the choice of unit cell only affects how we represent the same aperture function  $t(\xi, \eta)$  and their PSFs remain the same naturally. Nevertheless, it is enlightening that optimizing the pixel structures within a unit cell  $t_0(\xi, \eta)$  containing several pixels could possibly decrease the diffraction intensity. Here, the coordinates of the opaque regions in each pixel are the optimization variables and the diffraction intensity is the objective functions. The vertical coordinates in each row and horizontal coordinates in each column should stay the same for the ease of circuit layout and fabrication. This restriction greatly reduces the optimization variables from  $2n^2$  to  $2n$  for a unit size with  $n\times n$  pixels.

In the global optimization, the unit cell sizes are set by pixel number in one dimension  $n=1\sim 10$  and the aperture ratios are set to  $\alpha=30\%$ ,  $50\%$  and  $70\%$ . The optimized diffraction efficiencies at each case are plotted in Figure 5. As the pixel number  $n$  increases, the diffraction efficiency decreases and gradually converges to a stable value for each aperture ratio. Before optimization, the diffraction intensities for each aperture ratio are 0.19, 0.13 and 0.06 and they drop to 0.15, 0.05 and 0.01 after

optimization, where the relative diffraction intensity drops are 21%, 62% and 83%. When pixel number  $n=1$ , the diffraction intensities are the same as those in an unoptimized structure due to periodicity. The diffraction intensity of an optimized pixel structure with  $\alpha=50\%$  is even lower than that of an unoptimized structure. By optimizing pixel structures in unit cells with  $n=2$ , the diffraction effect has been greatly mitigated, and the relative diffraction drops are 21%, 42% and 58% at each aperture ratio. One of the optimized cell unit pixel structures  $t_0(\xi, \eta)$  for  $n=3$  and  $\alpha=50\%$  is shown in Figure 6(a) and its FT  $h_0(x, y)$  and horizontal cross section  $h_0(x, 0)$  is plotted in Figure 6(b)(c). Compared with the unoptimized structure, the energy distribution in the optimized pixel structure avoids its peaks to be coincided with the position of diffraction orders, leading to an effectively lower diffraction intensity.

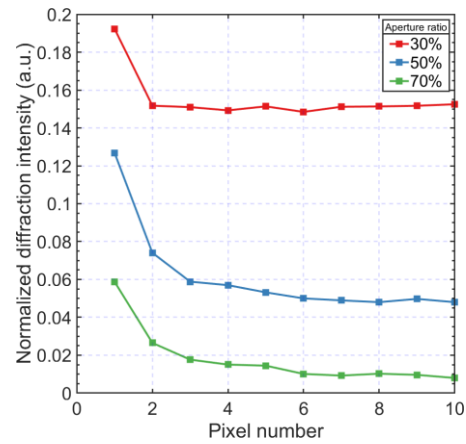


**Figure 5.** Global optimization result of diffraction intensities with unit cell sizes  $n=1\sim 10$  and aperture ratios  $\alpha=30\%$ ,  $50\%$  and  $70\%$ .

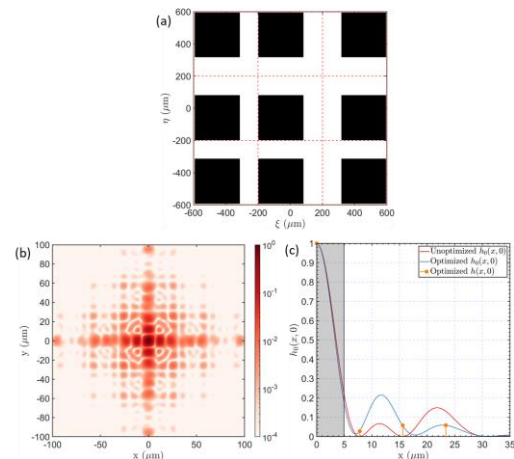


**Figure 6.** (a) An optimized pixel structures within a unit cell with  $3\times 3$ -pixel size and aperture ratio  $\alpha=50\%$ . (b) FT of the optimized structure. (c) Horizontal cross section  $h_0(x, 0)$  of the optimized and unoptimized structures and PSF  $h(x, 0)$  of the optimized structure.

With the aid of PSF, diffracted images of background objects could be obtained by convoluting ideal images under geometric optics with PSF, assuming the display panel is viewed on-axis. For real objects, diffracted images at visible light wavelengths (400nm-760nm) are synthesized into a hyperspectral image and converted to a RGB image, with reflected spectrum as weighting

coefficients. The accuracy of this method is experimentally verified in [9]. To intuitively illustrate the diffraction-suppression effect of our optimized pixel structures, three letters 'UCF' are used as our background object, shown in Figure 7(a). We assume  $d_2=25\text{cm}$  and the object size is  $50\text{mm}\times 38\text{mm}$ , located  $1\text{m}$  away from the observer. Image blur effect with unoptimized structure is displayed in Figure 7(b). Figure 8 shows the improvement of image quality with our optimized pixel structures. The diffraction is greatly suppressed with a  $2\times 2$ -pixel unit cell, comparing Figure 8(d) with Figure 8(e).

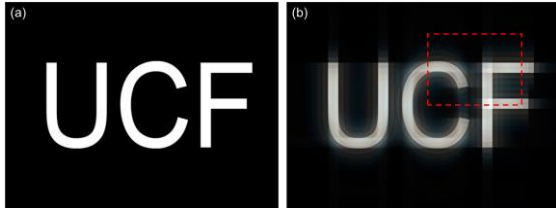


**Figure 7.** (a) Test background object. (b) Diffracted image with unoptimized pixel structure at 30% aperture ratio.

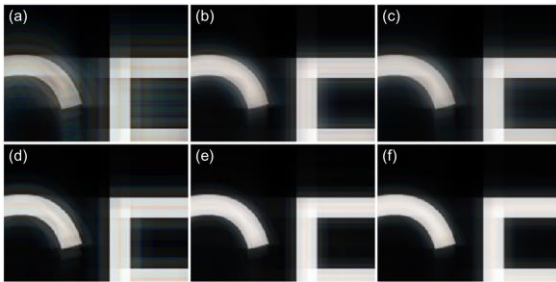


**Figure 8.** Diffracted images at aperture ratio 30% (a-c) and 50% (d-f) with unit cell sizes  $n=1,2,3$ .

## 5. Conclusion

We build a simple and reference image independent model to quantitatively evaluate the diffraction effect of the transparent display to human eyes. Based on diffraction theory, the PSF of the imaging system including the transparent display aperture function and a human eye is derived and the relative diffraction intensity is used as the metric to characterize the diffraction effect, with the angular resolution of human eyes considered. The impact of object distance, panel resolution and pixel aperture ratio to the diffraction intensity is analyzed in the conventional pixel structures. As a result, the object at infinity suffers the most from diffraction. A larger aperture significantly reduces diffraction intensity, while the resolution plays a trivial role. The aperture function of the transparent display is regarded as a 2D grating, which can be segmented as the convolution of a unit cell function and a comb function. By optimizing the pixel structures within unit cells with  $2\times 2$ -pixel size, the relative diffraction intensity drops 42% at 50% aperture ratio, equivalent to that of the unoptimized pixel structure with 70% aperture

ratio. This paper proposed a simple and achievable method for suppressing the diffraction effect in a transparent display by slightly tweaking the pixel structure, which is valuable for the industry since high aperture ratio and high pixel density panels are difficult to achieve simultaneously with current fabrication capability.

## 6. Acknowledgements

We are indebted to a.u.Vista, Inc. for funding support. We would like to thank En-lin Hsiang and Jianghao Xiong for valuable discussions.

## 7. References

1. Wager JF. Transparent electronics. *Science*. 2003 May 23;300(5623):1245-1246.
2. Xiong J, Hsiang EL, He Z, Zhan T, Wu ST. Augmented reality and virtual reality displays: emerging technologies and future perspectives. *Light: Science & Applications*. 2021 Oct 25;10(1):216.
3. Huang Y, Hsiang EL, Deng MY, Wu ST. Mini-LED, Micro-LED and OLED displays: Present status and future perspectives. *Light: Science & Applications*. 2020 Jun 18;9(1):105.
4. Liu YT, Liao KY, Lin CL, Li YL. 66 - 2: Invited Paper: PixeLED Display for Transparent Applications. *SID Symposium Digest of Technical Papers*. 2018 May; 49(1):874-875.
5. Biwa G, Aoyagi A, Doi M, Tomoda K, Yasuda A, Kadota H. Technologies for the Crystal LED display system. *Journal of the Society for Information Display*. 2021 Jun;29(6):435-445.
6. Goodman, JW. *Introduction to Fourier Optics*. New York: McGraw-Hill. 1996.
7. Zhou Y, Ren D, Emerton N, Lim S, Large T. Image Restoration for Under-Display Camera. *Proceedings of the IEEE/CVF Conference on Computer Vision and Pattern Recognition*. 2021;9179-9188.
8. Tsai YH, Huang MH, Huang TW, Lo KL, Ou-Yang M. Image quality affected by diffraction of aperture structure arrangement in transparent active-matrix organic light-emitting diode displays. *Applied optics*. 2015 Oct 1;54(28):E136-E145.
9. Qin Z, Xie J, Lin FC, Huang YP, Shieh HP. Evaluation of a transparent display's pixel structure regarding subjective quality of diffracted see-through images. *IEEE Photonics Journal*. 2017 Jun 30;9(4):1-14.